Characterization of a silicon-related defect detected by its excited triplet state in electron-irradiated 3C-SiC

Jérémie Lefèvre,[1] Jean-Marc Costantini,[2,*] Didier Gourier,[3] Stéphane Esnouf,[1,†] and Guillaume Petite[1]

[1]*Laboratoire des Solides Irradiés, École Polytechnique, CEA-IRAMIS, CNRS, F-91128 Palaiseau Cedex, France*

[2]*CEA, DEN, SRMA, F-91191 Gif-sur-Yvette Cedex, France*

[3]*Laboratoire de Chimie de la Matière Condensée de Paris, UMR-CNRS 7574, École Nationale Supérieure de Chimie de Paris (Chimie-ParisTech), 11, rue Pierre et Marie Curie, 75231 Paris Cedex 05, France*

(Received 27 March 2010; revised manuscript received 29 December 2010; published 22 February 2011)

Using electron paramagnetic resonance (EPR) under band-gap illumination, we show experimental evidence of a defect center in *n*-type cubic silicon carbide (3C-SiC) single crystal irradiated with 1-MeV electrons. This defect is diamagnetic ($S = 0$) in its ground state and can be pumped into a paramagnetic ($S = 1$, $M_S = 0$) state by above-band-gap photon excitation, where it is detected by EPR absorption and emission transitions $M_S = 0 \leftrightarrow M_S = \pm 1$. This defect is characterized by $g = 2.0029$, a zero-field splitting $D = 24.6 \times 10^{-4}$ cm^{-1}, and a hyperfine interaction $A = 2.61 \times 10^{-4}$ cm^{-1}. By studying the annealing behavior of this defect localized at a silicon site, we suggest that it is associated with the neutral silicon vacancy.

DOI: 10.1103/PhysRevB.83.075201 PACS number(s): 61.72.J−

I. INTRODUCTION

Silicon carbide (SiC) is a very promising material for semiconductor device applications, which have to work under extreme conditions. Due to its good thermal conductivity, high radiation resistance, and high breakdown voltage, it is well suited for demanding applications in harsh environments.[1] Even though progress in crystal growth during the past years has been able to reduce imperfections in SiC to a great extent, many properties of native defects or those produced by irradiation damage are still not well understood.

This paper focuses on a primary defect in SiC, which is produced by high-energy particle bombardment. If the energy of these particles is high enough, atoms in the lattice can actually be kicked out of their sites. The primary defects created in this way are generally vacancies and interstitials, but in a binary compound like SiC, antisites can also be formed. Therefore, a good knowledge of primary defects is especially important for SiC. The bombardment of the material with electrons or heavy ions creates a lot of defects in the material. In contrast to silicon, these defects are stable in silicon carbide at room temperature (RT),[2–5] and some secondary defects produced during a post-irradiation thermal annealing are stable at least up to 2000 °C,[4,6] that is, it is almost impossible to get rid of them. They can be easily studied with a variety of experimental techniques. Among these, electron paramagnetic resonance (EPR) allowed us to identify a large number of intrinsic point defects in SiC, as summarized in Table I for the most common hexagonal polytypes (4H, 6H) and for the cubic structure (3C).

EPR data were assigned to the $V_{Si}Si_i$ Frenkel pair in the silicon sublattice of 300-keV electron irradiated 6H-SiC single crystals.[7,8] The charge state of this defect seems to be dependent on the initial doping of the material, since these authors suggested the one- and three-charge states in *n*-type and *p*-type samples, respectively.

The negatively charged silicon vacancy V_{Si}^- is a well-known defect in 4H- and 6H-SiC.[3,9–13] Basically, it is similar to the V^- center in diamond by its high spin ($S = 3/2$) ground state.[14] The effective spin $S = 3/2$ of V_{Si}^- in 4H-SiC was confirmed by pulsed electron-nuclear double resonance (ENDOR) measurements.[11] The signal of V_{Si}^0 in hexagonal and cubic sites was observed in addition to that of V_{Si}^- in *n*-type 4H and 6H-SiC irradiated with high-energy protons (12 MeV) for fluences ranging from 1×10^{16} to 8×10^{16} cm^{-2}.[15] The lack of signal related to the nitrogen donor at low temperature, associated with the simultaneous presence of the two charge states of the silicon vacancy, indicates that irradiated crystals are electrically compensated regardless of fluence. In proton-irradiated *n*-type 6H-SiC samples at higher fluences, the ionization level (−/0) of the silicon vacancy seems to govern the position of the Fermi level, which is located close to the middle of the gap.

The T_{V2a} center can be detected by photoluminescence (PL), which is called the *V*2 line (1.352 eV). The equivalence of T_{V2a} and *V*2 was demonstrated by optically detected electron magnetic resonance (ODMR).[11,13] The determination of the spin state $S = 3/2$ of the T_{V2a} center by the nutation method in pulsed EPR has revealed that T_{V2a} belongs to a family of V_{Si}^-. The complete analysis of the T_{V2a} spectrum was achieved by using the signal enhancement due to electron-spin polarization by light illumination.[11,16] However, the central primary line of T_{V2a} was often missing, because it was not enhanced by illumination and was usually hidden underneath the v_{Si}^- signal. This led to the mistaken idea that T_{V2a} originates from v_{Si}^0 with $S = 1$.[16]

The carbon vacancy is also a well-known primary defect in SiC, which was essentially observed in its positive charge state (V_C^+, $S = 1/2$) by EPR in *p*-type 4H and 6H polytypes irradiated with electrons. The EI5 and EI6 centers, found in the 4H polytype,[5,17,18] have been established to be V_C^+ at cubic (*k*) and hexagonal (*h*) sites, respectively. Similarly, the Ky1/2 and Ky3 centers in 6H-SiC have been identified as V_C^+ at two cubic sites (*k*1, *k*2) and one hexagonal site, respectively.[19] In 4H-SiC, the negatively charged carbon vacancy (V_C^-, $S = 1/2$) was also found.[20]

EPR and *ab initio* supercell calculations suggest that the P6/P7 centers, which were previously assigned to the

TABLE I. Point defects identified by EPR measurements in 3C, 4H, and 6H-SiC irradiated with electrons (e^-), protons (H^+), or neutrons (n). We mention which assignment has been already confirmed by theory (theor) or proposed by experimentalists (expt).

Point	Polytype	EPR signal	Incident particle	Irradiation energy	Reference
defect	(doping)			(MeV)	
$(V_{Si}Si_i)^-$ (expt)	6H (p)		e^-	0.3	7
$(V_{Si}Si_i)^{3-}$ (expt)	6H (n)		e^-	0.35	8
V_{Si}^-	3C (n), (p)	T_1	e^-,H^+	1, 2	29–31
(theor)	4H (n)		n, e^-	>0.1, 3	10,11
	6H (n)		e^-	3	9,12
	4H, 6H	T_{V2a}	e^-	3	11,13
V_{Si}^0 (theor)	4H (n)		H^+	12	15
	6H (n)		H^+	12	15
V_C^+ (theor)	4H (p)	EI5, EI6	e^-	2.5	5,17,18
	6H (p)	Ky1, Ky2, and Ky3	e^-	2	19
V_C^- (theor)	4H (n)	HEI1	e^-	3.5	20
$(V_{Si}V_C)^0$ (theor)	4H, 6H	P6/P7	e^-	2.5	23
C_{Si} (theor)	6H (n)		n	1	24
$(C_2)_{Si}^-$ (theor)	4H (n)	HEI5, HEI6	e^-	3	25
$(V_CC_{Si})^+$ (theor)	4H (p)	HEI9/10	e^-	3	26
$(V_CC_{Si})^-$ (theor)	4H (n)	HEI4/SI-5	e^-	3	27
$(Si_CC_{Si})^+$	3H (n), 6H (p)		H^+	6.3	28
(th)	4H (p)		H^+	from 0.35 to 1	28
$(V_{Si}Si_i)^{3+}$ (theor)	3C (n)	LE1	e^-	2	32

photoexcited triplet states of the carbon vacancy–antisite pairs in the double positive charge state,[21,22] are related to the triplet ground states of the neutral divacancy $(V_{Si}V_C)^0$.[23] The spin density is found to be located mainly on three nearest C neighbors of the silicon vacancy, whereas it is negligible on the nearest Si neighbors of the carbon vacancy.

An EPR spectrum with axial symmetry along the c axis, spin $S = 1/2$, and strong hyperfine interaction with one carbon atom has been observed in neutron-irradiated and annealed 6H-SiC,^{13}C isotope enriched.[24] The spectrum was identified as arising from an isolated carbon atom presumably in Si position, C_{Si}.

Umeda *et al.*[25] identified the negatively charged dicarbon antisite defect $(C_2)_{Si}^-$ in electron-irradiated n-type 4H-SiC by means of combined EPR measurements and first- principles calculations. The HEI5 and HEI6 EPR centers ($S = 1/2$; C_{1h} symmetry) are associated with cubic and hexagonal dicarbon antisite defects, respectively. This assignment is based on a comparison of the measured and calculated hyperfine tensors of^{13}C and ^{29}Si atoms as far as the second neighborhood around the defects. Theoretically, the dicarbon antisites are stable in a single negative charge state under a wide range of n-type samples.

The identification of the missing positively charged carbon antisite–vacancy pairs $(V_CC_{Si})^+$ has been assessed by means of *ab initio* supercell calculations.[26] These defects were also detected in the negatively charged states.[27]

Very recently, the nearest-neighbor antisite pair defects in 4H-SiC, 6H-SiC, and 3C-SiC single crystals have been identified using EPR spectroscopy in combination with a nonperturbative *ab initio* scheme for the electronic g tensor.[28] Based on the theoretical predictions, the positively charged defect has been found experimentally also in the cubic 3C-SiC polytype where it is characterized by spin 1/2 and highly anisotropic g values of $g_{xx} = 2.0030$, $g_{yy} = 2.0241$, and $g_{zz} = 2.0390$ within C_{1h} symmetry. The exceptional large g values are explained by details of the spin-orbit coupling causing a strongly anisotropic quenching of the orbital angular momentum of the p-like unpaired electron.

Only a few studies have been done in the cubic polytype (3C-SiC) because of the difficulty in obtaining high-quality materials. The negatively charged silicon vacancy (T_1 center) was identified in n-type epilayers.[29,30] The T_d symmetry of this defect was confirmed by the angular dependence of ^{13}C hf lines of the nearest neighbors. In the T_d symmetry, all three $\Delta M_S = \pm 1$ transitions of $S = 3/2$ are superimposed since the zero-field splitting (ZFS) vanishes in cubic symmetry. In a recent study, we deduced the threshold displacement energy in the Si sublattice [E_d(Si)] from PL and EPR data of V_{Si}^- in n-doped electron-irradiated 3C-SiC single crystals.[4] Concerning p-type crystals, Itoh *et al.*[31] simultaneously discovered the negatively charged silicon vacancy, the carbon di-interstitial defect $(C_{sp})_2^+$, and two signals characterized by a dipole-dipole interaction and attributed to vacancy-interstitial pairs.

The $(V_{Si}Si_i)^{3+}$ Frenkel pair has been identified in n-type 3C-SiC after electron irradiation at low temperature (80–100 K).[32] The LE1 signal related to this defect, observed at low temperature, disappears after warming up the samples to RT. Supercell calculations of different configurations of silicon vacancy-interstitial Frenkel pairs were performed showing that pairs with a nearest-neighbor Si interstitial are unstable whereas pairs with a second-neighbor Si_i are stable. Comparing the data obtained from EPR and supercell calculations, the LE1 center is assigned to the Frenkel-pair between V_{Si} and a second-neighbor Si_i interstitial along the [100] direction in the 3+ charge state, $(V_{Si}Si_i)^{3+}$. This important result shows that

in materials irradiated at low temperatures, Frenkel pairs are dominating defects whereas EPR signals of single vacancies are absent.

The present work specifically deals with photo-EPR measurements performed in an *n*-type 3C-SiC single crystal irradiated with 1-MeV electrons. After a brief description of the experimental protocol, we characterize the properties of an EPR-active center. From these results, the electronic structure of the defect is discussed and a defect model is proposed.

II. EXPERIMENTAL PROCEDURE

The material investigated in this study was supplied by the HOYA Company. This is a [100]-oriented 3C-SiC single crystal grown epitaxially on a crystalline Si [111] substrate by chemical vapor deposition. The sample characterized by EPR measurements is 157-μm-thick with a free-carrier concentration ($N_D - N_A$) of 8.4×10^{15} cm^{-3} due to nitrogen donors. By use of a HF/HNO_3 1:1 solution, the Si substrate was completely etched away. The single crystal was finally polished at RT at the NOVASiC Company by a mechanochemical process.

An irradiation at 300 K with 1-MeV electron at a fluence of 1.3×10^{18} cm^{-2} was carried out along the [100] crystallographic direction using a Van-de-Graaff accelerator at the Laboratoire des Solides Irradiés (LSI, École Polytechnique, Palaiseau). The electron flux was kept below 1.8×10^{14} cm^{-3} s^{-1} to minimize the sample heating. In the present study, we have used a single fluence for which a high number of paramagnetic centers (negative silicon vacancy) are produced. By varying the electron fluence, we showed previously that the threshold displacement energy (E_d) in the silicon sublattice is equal to 25 eV along the [100] axis.[33] Considering an E_d value of 20 eV in the carbon sublattice,[34] calculations performed with SMOTT, POLY, and PENELOPE computer codes suggest that the defect formation is quite homogeneous throughout the sample thickness, the electrons being transmitted through the samples.[35,36]

The photo-EPR measurements were performed in a Bruker ESP 300e X-band EPR spectrometer (operating at 9.6 GHz) equipped either with a 3 kW high-pressure mercury vapor lamp combined with interference filters for a wavelength range of 380–1000 nm, or with a frequency-doubled YVO_3:Nd^{3+} laser operating at 530 nm. Spectra were fitted with different Lorentzian- and Gaussian-shaped components. The concentrations of the various paramagnetic centers in the whole irradiated crystal were determined by comparison with a $CuSO_4$ reference sample.

III. RESULTS

The EPR spectra of the electron-irradiated sample recorded at 100 K, in the dark and under laser illumination, are shown in Fig. 1, when the static magnetic field is applied perpendicularly to the [100] axis of the single crystal. Before photoexcitation [Fig. 1(a)], the EPR signal exhibits the well-known T_1 center, which is formed by a central line with a hyperfine (hf) structure. This signal is attributed to V_{Si}^- with an effective spin $S = 3/2$.[29] The defect concentration is estimated to be 2.5×10^{16} cm^{-3}, which is in quite good agreement with a production rate of 1.7×10^{-2} cm^{-1} in 3C-SiC irradiated with 1-MeV electrons.[29] Two sets of lines split by 2.88 mT appear under light illumination at 1 W cm^{-2}, with significant microwave attenuation to 50 dB [Fig. 1(b)]. Such a signal, arbitrarily labeled as T_X, has not been previously observed in 3C-SiC, either in *n*-type or *p*-type materials. It is detected at 4 K but the best temperature interval for the observation of this new EPR center is between 100 and 200 K. Indeed, the signal saturates below 100 K and its hyperfine structure cannot be resolved any further, whereas its intensity decreases drastically above 200 K.

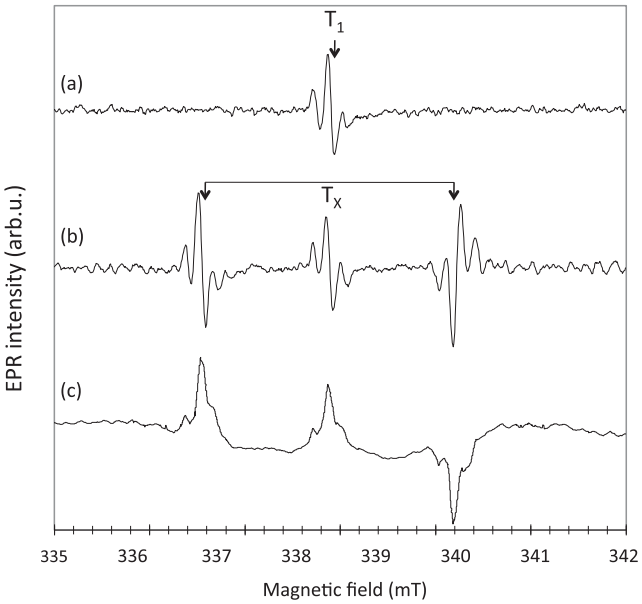

FIG. 1. First derivative of the EPR spectrum at 100 K with B ⊥ [100] of the *n*-type 3C-SiC sample irradiated with 1-MeV electron in the dark (a) and under light illumination (b). In the latter case, a new signal referred to as T_X is observed. (c) Integration of the spectrum (b) [microwave attenuation = 50 dB (1 mW), modulation depth = 0.3 G)].

Considering, for example, the low-magnetic-field component of the T_X signal [Fig. 1(b)], we notice a symmetric structure composed by a series of five lines with a splitting of 144 μT. These are labeled *a* for the central line, *b* for the two first adjacent ones, and *c* for the two weak satellites (see Fig. 2). The a/b and a/c ratios are equal to (0.274 ± 0.03) and (0.035 ± 0.004), respectively, which correspond to the hf interaction of an unpaired electron with 12 neighboring silicon isotopes (^{29}Si: $S = 1/2$, abundance 4.7%). The relative intensity of the *b* line compared to *a* is indeed 12 times higher than the relative abundance of ^{29}Si. Besides, the central line *a*, with a linewidth of 92 μT, and the *b* and *c* doublets are correctly fitted by an interaction with zero, one, and two ^{29}Si nuclei in sites corresponding to the 12 equivalent neighboring silicon atoms (Fig. 2). The experimental value of the hf interaction $|A_{Si}|/g_N\mu_N$ (Fig. 2) is equal to 287.3 μT (i.e., 2.61×10^{-4} cm^{-1}). This value is close to that found for the negatively charged silicon vacancy V_{Si}^- (2.73×10^{-4} cm^{-1}). The ^{29}Si hf interaction in 12 equivalent silicon sites clearly demonstrates that the T_X center arises from a defect at a silicon site. Moreover, in spite of numerous signal accumulations, it was not possible to identify any hf interaction with ^{13}C atoms.

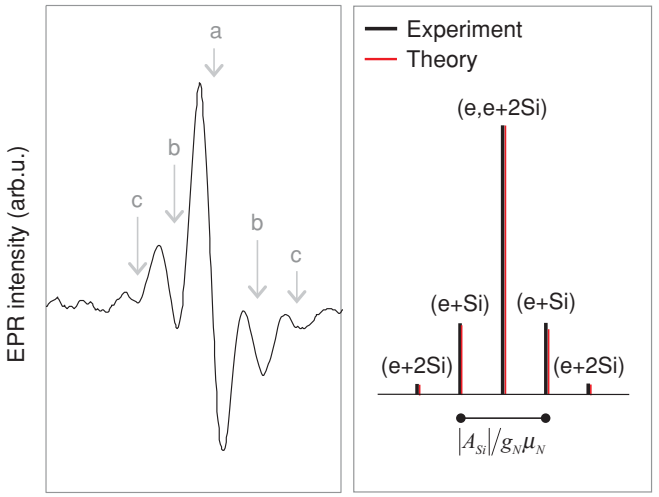

FIG. 2. (Color online) Left: low-field component of the T_X signal with B ⊥ [100]. Right: corresponding stick diagram calculated from hyperfine interactions of an electron with zero, one, and two ^{29}Si nuclei located in 12 equivalent silicon sites.

This may be due to a strain broadening effect of the weak ^{13}C hf lines, produced by the mechanical stress on the 3C-SiC crystal resulting from the growing procedure on the Si substrate.

From the integration of the first derivative EPR spectrum (Fig. 1(c)), it can be seen that the low-magnetic-field component of the signal results from a microwave absorption, while the high-field component originates from a microwave emission, indicating that we are faced with an out-of-equilibrium population of the spin states of this defect. To explain the nature of this EPR signal, we performed a series of additional measurements. First, we have to check that the two components of the T_X doublet are related to the same point defect. Second, we have to confirm that the signal T_X does not correspond to V_{Si}^- in an excited state. Third, we must verify that no additional line associated with the new EPR center is superimposed with the T_1 spectrum.

Intensities (in arbitrary units) of the T_1 and T_X signals are compared for different illumination values (Fig. 3). Actually, since the T_X center is only observed by optical excitation, the population of the Zeeman levels of this defect is highly in nonequilibrium, in contrast to the T_1 center. Hence, it is not possible to compare the intensities of the T_X and T_1 signals, and no absolute concentration values of the T_X center can reliably be given. Between each measurement taken during a similar time interval, the sample was kept in the dark for 15 min. Results show that the intensity of the low- and high-field components of T_X jointly increase with illumination up to saturation at 1.25 W cm^{-2}. This behavior is reversible since a decrease of illumination implies an immediate decrease of the intensity of the T_X signal. Besides, we notice that T_1 is not affected during measurements. These observations show that the spectrum of T_X is only formed by two sets of lines related to a unique point defect, distinct from the negatively charged silicon vacancy V_{Si}^-.

Information about the electronic structure of the defect associated with T_X is obtained from the angular dependence measurements in the (011) plane of the crystal. Figure 4 illustrates the behavior of the central line (a) for each of the two

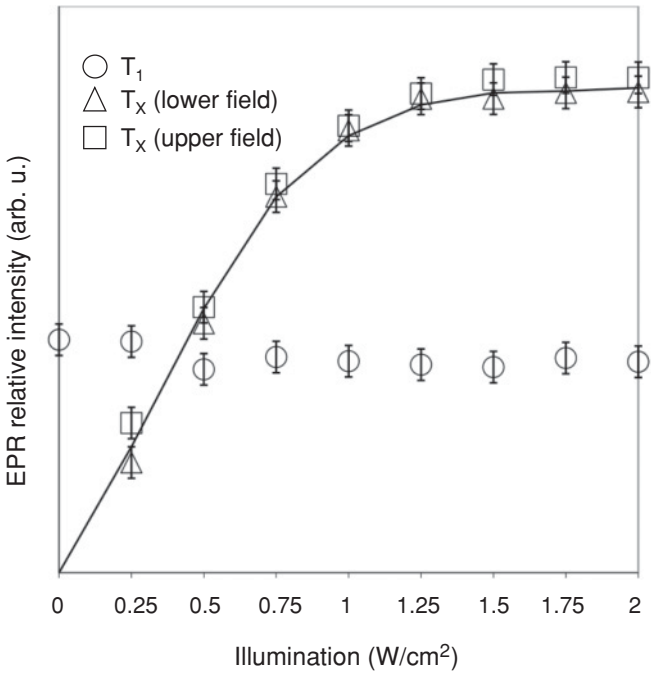

FIG. 3. EPR intensities vs light intensity of the T_1 center (circles) and of the two components of T_X corresponding to microwave absorption at low magnetic field (triangles) and microwave emission at high field (squares).

components of T_X as a function of the angle ($\vec{B_0}$,[100]) formed by the static magnetic field $\vec{B_0}$ and the crystalline direction [100]. Owing to line broadening, it was not feasible to follow the angular variation of the ^{29}Si hf interaction because it was unresolved when B_0 deviates from the [100] axis.

The splitting of a lines is maximum when $\vec{B_0}$ is aligned along [100], vanishes when the magnetic is parallel to the

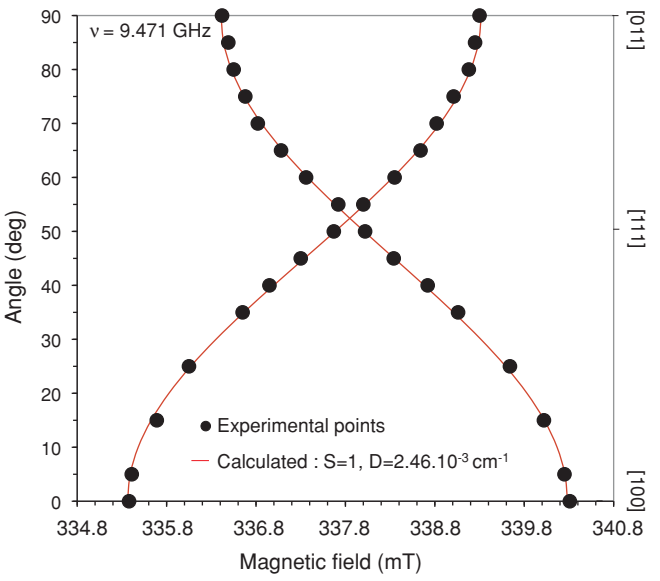

FIG. 4. (Color online) Angular dependence of the central line (a) of the T_X signal. The angle is calculated between the magnetic field and the [100] crystalline axis. The full line corresponds to the angular dependence calculated with Eq. (1) for $D = 2.46 \times 10^{-3}$ cm^{-1}.

[111] ternary axis, and is half the maximum value when $\overrightarrow{B_0}$ is aligned along the [011] axis. This behavior is typical for a traceless tensor such as the ZFS of an $S = 1$ state. The angular dependence of the resonance field B_{res} of the central lines (corresponding to 100 % neighboring ^{28}Si nuclei) can thus be written as

$$B_{\text{res}} = \frac{1}{g\mu_B}\left(h\nu \pm \frac{D}{2}[3cos^2\theta - 1]\right), \qquad (1)$$

where the isotropic g factor is equal to 2.0029 ± 0.0001, μ_B defines the electronic Bohr magneton, D describes the ZFS, and θ represents the angle between $\overrightarrow{B_0}$ and the [100] main axis of the 3C-SiC crystal. For T_X centers with one and two neighboring ^{29}Si nuclei, a hf term must be added in Eq. (1). The angular dependence of the central line is typical of a spin-triplet state $S = 1$ with an axial zero-field splitting $D =$ 26.38 MHz (i.e., 24.6 × 10^{-4} cm^{-1}). For some orientations, we observe two additional line doublets with profiles similar to those observed in Fig. 1, due to the cubic symmetry of the crystal. However, the angular dependence of the ^{29}Si hyperfine lines could not be recorded because of the weakness of the associated signal during the angular variation experiment. As for ^{13}C hf lines, this likely originates from the strain broadening effect due to the Si substrate.

We report in Fig. 5 the excitation spectrum of the T_X center taken with the mercury vapor lamp. For each wavelength, we adjusted the incident power density so that the illumination received by the sample was kept constant during measurements. We notice that photon energy equal to or larger than 2.23 ± 0.05 eV is necessary to observe the T_X spectrum. The intensity

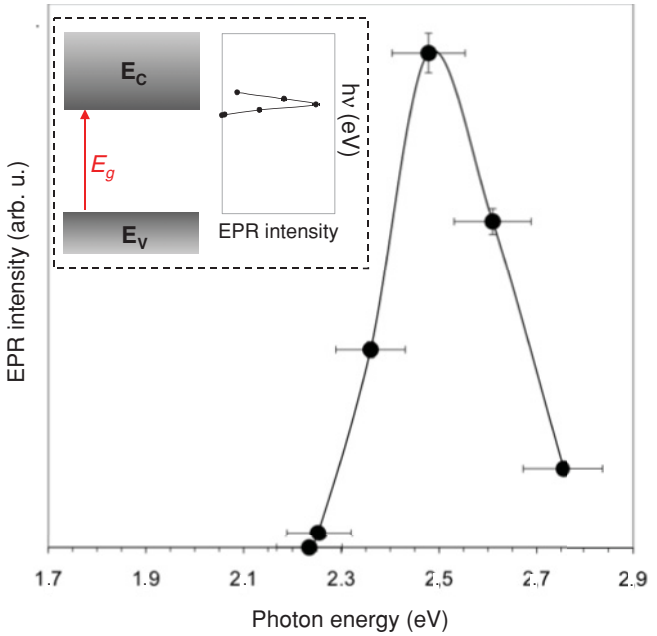

FIG. 5. (Color online) Excitation spectrum of the T_X center taken at 100 K using the mercury vapor lamp. Inset: the photon energy emitted from the light source is plotted as a function of the EPR intensity and compared to the band-gap value (E_g) of 3C-SiC, equal to 2.391 eV at 100 K (Ref. 37).

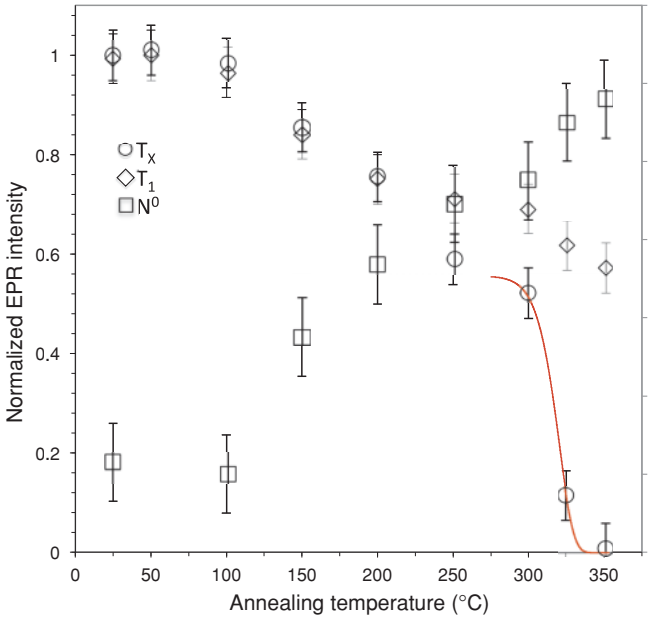

FIG. 6. (Color online) Variations with annealing temperature (T) of the intensities (I) of the T_1 (diamonds), T_X (circles), and N^0 signals (squares), normalized to the initial values (I_0) recorded at 300, 100, and 30 K, respectively. The red curve corresponds to the best fit of the experimental points with Eq. (2).

of the signal increases up to a maximum at 2.55 ± 0.04 eV and then decreases for higher-energy values.

The annealing behavior of T_X, T_1 and the nitrogen (N^0) signals is compared in Fig. 6. Let I_0 be the intensity recorded at low temperature before annealing and $I(T)$ be the intensity measured after isochronal annealing at the temperature T. We observe that the annealing behavior of the defect related to T_X is divided into two stages. The first one, ranging between 100 and 250 °C, leads to a decrease of 35% of the initial signal intensity. The second step, initiated at around 300 °C, implies the annihilation of the EPR center at 350 °C. This annealing kinetic is qualitatively similar to that of T_1 center. The concentration of negative silicon vacancies (T_1) decreases by about 30% at 200 °C and then 15% at 350 °C. The partial restoration of the N^0 signal is correlated with the annealing behavior of T_1 (Fig. 6). Indeed, 30% and 40% of the original concentration of free carriers are recovered after isochronal annealing at 250 and 350 °C, respectively. Therefore, it seems that the T_X center does not play any role in the electrical compensation of the sample. Besides, a good fit of the experimental points, obtained with a sigmoid curve of first order, allows us to evaluate the activation energy $E_a = 1.37 \pm 0.15$ eV for the thermal bleaching of the T_X center above 250 °C:

$$I/I_0 = \exp[-\nu_0 t_a \exp(-E_a/k_B T)], \qquad (2)$$

where I is the EPR intensity, I_0 is the value obtained prior to the annealing experiment, ν_0 is a frequency factor, t_a is the annealing time (1800 s), k_B is the Boltzmann constant, and T is the annealing temperature.

IV. DISCUSSION

This photo-EPR experiment allowed us to identify a new center, labeled T_X, with characteristics summarized in Table II. It has not been observed either in samples irradiated at RT with electrons below E_d(Si),[33] or in materials irradiated with 12-MeV protons or with 132-MeV C^+ ions at fluences ranging from around 2×10^{14} to 4×10^{16} cm^{-2}.

The angular dependence of the EPR lines (Fig. 4) shows that it is associated with a point defect in an excited triplet spin state ($S = 1$). As illustrated in Fig. 7, the EPR transitions between the M_S sublevels are $|S,M_S\rangle = |1,0\rangle \leftrightarrow |1,+1\rangle$ and $|S,M_S\rangle = |1,0\rangle \leftrightarrow |1,-1\rangle$ according to the selection rule $\Delta M_S = \pm 1$. The observation of an absorption signal at low magnetic field and of an emission signal at high magnetic field shows that the $|1,0\rangle$ spin state is more populated than the $|1,-1\rangle$ and $|1,+1\rangle$ ones, implying that the three states are not in thermal equilibrium under illumination.

The direct optical transition from the $S = 0$ ground state to a triplet state $S = 1$ is forbidden according to the electric-dipole selection rule $\Delta S = 0$. Thus the out-of-equilibrium population of the excited $|S,M_S\rangle = |1,0\rangle$ state is due to a more complicated process, as illustrated in Fig. 7. It starts with an optical transition from the ground state 1 to an excited state 3, both with a spin $S = 0$, followed by an intersystem crossing to the excited triplet state $S = 1$ (level 2). The emission toward the ground state is spin forbidden, so that the radiative lifetime $\tau_{\rm rad}$ is sufficiently large to allow the observation of the excited triplet state by EPR. However, a weak radiative transition to the singlet ground state $|0,0\rangle$ is allowed from the $|1,+1\rangle$ and $|1,-1\rangle$ states, but not from the $|1,0\rangle$ state.[38] Therefore, the excited state $|1,0\rangle$ will maintain a higher population, provided the spin lattice relaxation time T_1 is larger than $\tau_{\rm rad}$. According to this population difference, the microwave field of EPR will induce a microwave absorption $|1,0\rangle \rightarrow |1,+1\rangle$ and a microwave emission $|1,0\rangle \rightarrow |1,-1\rangle$. The fact that this population difference can be maintained implies also that the excited triplet state (level 2) is not resonant with the conduction band, and lies in the band gap, otherwise we expect a loss of spin memory while the electrons thermalize in the band. It should be noticed that such out-of-equilibrium population of the $|S = 1, M_S = 0, \pm 1\rangle$ excited states is one of the mechanisms of optical detection of EPR. For example, the EPR of the F center (F^0 : neutral oxygen vacancy) in CaO has been optically detected via the microwave-induced change of the triplet-state phosphorescence.[38] By modifying the out-of-equilibrium populations of the triplet state, the microwave induces a change of the emission intensities from the $|1,\pm 1\rangle$ states.

Remembering that the hf pattern indicates that this defect is located at a silicon site, and that the hf interaction and the g factors are very close to those of the T_1 center attributed to the V_{Si}^- defect, it appears likely that the T_X center is the neutral silicon vacancy defect V_{Si}^0. *Ab initio* calculations by Bockstedte *et al.*[39] performed in 3C-SiC within the framework of the density-functional theory localize the (0/+) ionization level of V_{Si} at $E_V + 0.18$ eV above the maximum of the valence band (E_V). A recent study using the multiconfigurational self-consistent-field method and taking into account the Jahn-Teller distortion shows that the ground state of V_{Si}^0 is a singlet spin state ($S = 0$) separated from the first excited state with $S = 1$ by about 0.1 eV.[40] Such an electronic configuration agrees with the energy-level scheme that we suggest for the T_X center (Fig. 7). Calculations indicate that the formation energy of this defect is slightly larger than the one estimated for V_{Si}^- under stoichiometric conditions. Indeed, Bockstedte *et al.*[41] calculated that the 1-charge state of the silicon vacancy prevails in n-type and compensated materials. After irradiation, the Fermi level may be pinned to the midgap position where the concentration of neutral and (1-) charged Si vacancy could be similar. Therefore, the involvement of V_{Si}^0 in the T_X signal appears likely.

TABLE II. Characteristics of the T_X center; $T_{\rm obs}$ and T_a correspond to the measurement and annealing temperatures, respectively. The negative sign of A corresponds to the nuclear momentum related to silicon.

g	S	D (cm^{-1})	$A_{\rm Si}$ (cm^{-1})	$T_{\rm obs}$ (K)	T_a (°C)
2.0029	1	24.6×10^{-4}	-2.61×10^{-4}	4→200	350

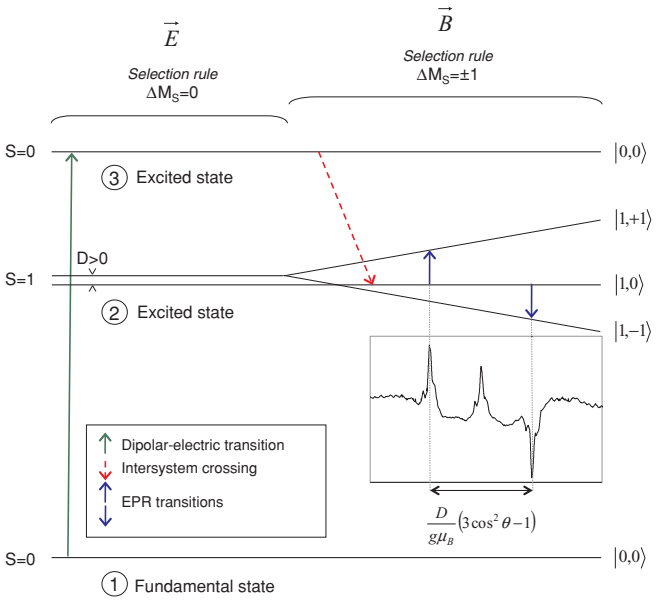

FIG. 7. (Color online) Suggested energy-level scheme for the T_X center.

Despite the fact that this interpretation agrees with the present observations and previous calculations, the attribution of the T_X center must be discussed in more detail because there are only a few studies dealing with the electronic structure of point defects in 3C-SiC,[32,42–47] and in particular we must eliminate other possible interpretations. Let us first consider extrinsic defects associated with N and H impurities, which are introduced into the lattice during the chemical-vapor-deposition growth. Concerning nitrogen, the electron spins should interact with the ^{14}N isotope ($I = 1$, abundance 99.64%) to induce an hf splitting forming a three-line pattern. Since no such signal has been observed in the T_X spectrum, we can reasonably exclude any implication of this impurity. In the case of hydrogen, electron spins should interact with the ^{1}H isotope ($I = 1/2$, abundance 99.38%) leading to a doublet hf pattern

similar to that observed for the T_X signal. The assumption of the diffusion of this impurity can thus be considered. However, a strong argument against this attribution is the fact that the splitting between the two sets of lines of the T_X center varies as $3\cos^2\theta - 1$ (i.e., it is a traceless interaction). In the case of a hydrogen-related defect, the hf interaction should contain a dominant Fermi contact contribution (which is isotropic) due to an unpaired electron spin density in the H 1*s* orbital, in addition to the traceless dipolar hf contribution. The lack of any isotropic contribution to the splitting of the T_X spectrum, which should dominate for a hydrogen impurity, definitely excludes the attribution of this defect to a hydrogen-related defect in silicon site.

This new EPR-active center is thus indisputably associated with an intrinsic point defect in 3C-SiC. Among all the species sitting on a silicon site, various antisite and interstitial defects can be created upon irradiation with 1-MeV electrons in addition to the silicon vacancy V_{Si}.[24,25,46,47] However, the assumption of these defects can reasonably be excluded due to the hyperfine splitting, which is characteristic of a silicon vacancy.[12]

We must point out that the T_X center exhibits a ZFS while this parameter should be exactly zero in the case of a vacancy V_{Si}^0 with T_d symmetry. A first possible cause of distortion from T_d to D_{2d} symmetry giving a ZFS could be the Jahn-Teller effect. The latter is not expected in the ^1E ground state of V_{Si}^0, which retains its T_d symmetry.[40] However, upon optically induced population of the long lifetime $^3T_1$ state giving the EPR spectrum, the Jahn-Teller distortion expected for such a state[48] should occur, giving a D_{2d} symmetry of the excited V_{Si}^0 center. A second possible origin for the ZFS is the symmetry-lowering resulting from a nonhomogeneous strain induced in the crystal by the Si substrate. Such strain is also responsible for the line broadening, which affects ^{13}C and ^{29}Si hf lines, as discussed above. These two mechanisms can combine to give the effective ZFS observed for the T_X center.

All the points discussed above lead us to conclude that the T_X-related center is most likely the neutral Si vacancy (V_{Si}^0).

V. CONCLUSIONS

Photo-EPR measurements in an *n*-type electron-irradiated 3C-SiC single crystal reveal a new signal labeled as T_X. It is composed of two sets of lines, which originate from microwave emission and absorption, respectively, showing out-of-equilibrium spin-state populations. We show that this signal is associated with an intrinsic defect in a long lifetime excited state with spin $S = 1$ located on the silicon sublattice.

We observed that its annealing kinetic is constituted by two stages at 150 and 350 °C, corresponding to the first two annealing stages of the silicon vacancy resulting from the recombination of Frenkel pairs in the silicon sublattice. According to calculations, we attribute the new T_X EPR center to the neutral silicon vacancy V_{Si}^0. Further investigations are needed to confirm this model.

ACKNOWLEDGMENTS

The authors sincerely thank Stéphane Guillous, Vincent Métayer, as well as Thierry Pouthier for their contributions during the irradiation experiments at the LSI. This work was supported by the CEA/CNRS research program ISMIR.

*jean-marc.costantini@cea.fr
†Present address: Laboratoire de Radiolyse, UMR-CNRS 3299, CEA-DSM-IRAMIS-SIS2M, F-91191 Gif-sur-Yvette Cedex, France.

[1] *Recent Major Advances in SiC*, edited by W. J. Choyke, H. Matsunami, and G. Pensl (Springer, Berlin, 2004), p. 437.
[2] H. Itoh, M. Yoshikawa, I. Nashiyama, S. Misawa, H. Okumura, and S. Yoshida, J. Electron. Mater. **21**, 707 (1992).
[3] H. Itoh, A. Uedono, T. Oshima, Y. Aoki, M. Yoshikawa, I. Nashiyama, S. Tanigawa, H. Okumura, and S. Yoshida, Appl. Phys. A **65**, 315 (1997).
[4] J. Lefèvre, J. M. Costantini, S. Esnouf, and G. Petite, J. Appl. Phys. **106**, 083509 (2009).
[5] N. T. Son, P. N. Hai, and E. Janzen, Phys. Rev. B **63**, 201201(R) (2001).
[6] W. J. Choyke, and L. Patrick, Phys. Rev. B **4**, 1843 (1971).
[7] H. J. von Bardeleben, J. L. Cantin, L. Henry, and M. F. Barthe, Phys. Rev. B **62**, 10841 (2000).
[8] H. J. von Bardeleben, P. Cantin, P. Baranov, and E. N. Mokhov, Mater. Sci. Forum **353-356**, 509 (2001).
[9] J. Schneider and K. Maier, Physica B **185**, 199 (1993).
[10] T. Wimbauer, B. K. Meyer, A. Hofstaetter, A. Scharmann, and H. Overhof, Phys. Rev. B **56**, 7384 (1997).
[11] N. Mizuochi, S. Yamasaki, H. Takizawa, N. Morishita, T. Ohshima, H. Itoh, and J. Isoya, Phys. Rev. B **66**, 235202 (2002).
[12] N. Mizuochi, S. Yamasaki, H. Takizawa, N. Morishita, T. Ohshima, H. Itoh, and J. Isoya, Phys. Rev. B **68**, 165206 (2003).
[13] N. Mizuochi, S. Yamasaki, H. Takizawa, N. Morishita, T. Ohshima, H. Itoh, T. Umeda, and J. Isoya, Phys. Rev. B **72**, 235208 (2005).
[14] J. Isoya, H. Kanda, Y. Uchida, S. C. Lawson, S. Yamasaki, H. Itoh, and Y. Morita, Phys. Rev. B **45**, 1436 (1992).
[15] H. J. von Bardeleben, J. L. Cantin, I. Vickridge, and G. Battistig, Phys. Rev. B **62**, 10126 (2000).
[16] M. Wagner, N. Q. Thinh, N. T. Son, W. M. Chen, E. Janzen, P. G. Baranov, E. N. Mokhov, C. Hallin, and J. L. Lindstrom, Phys. Rev. B **66**, 155214 (2002).
[17] T. Umeda, J. Isoya, N. Morishita, T. Ohshima, and T. Kamiya, Phys. Rev. B **69**, 121201(R) (2004).
[18] T. Umeda, J. Isoya, N. Morishita, T. Ohshima, T. Kamiya, A. Gali, P. Deak, N. T. Son, and E. Janzen, Phys. Rev. B **70**, 235212(R) (2004).
[19] V. Y. Bratus, T. T. Petrenko, S. M. Okulov, and T. L. Petrenko, Phys. Rev. B **71**, 125202 (2005).
[20] T. Umeda, Y. Ishitsuka, J. Isoya, N. T. Son, E. Janzen, N. Morishita, T. Ohshima, H. Itoh, and A. Gali, Phys. Rev. B **71**, 193202 (2005).
[21] T. Lingner, S. Greulich-Weber, J. M. Spaeth, U. Gerstmann, E. Rauls, Z. Hajnal, T. Frauenheim, and H. Overhof, Phys. Rev. B **64**, 245212 (2001).
[22] U. Gerstmann, E. Rauls, and H. Overhof, Phys. Rev. B **70**, 201204(R) (2004).
[23] N. T. Son, P. Carlsson, J. ul Hassan, E. Janzen, T. Umeda, J. Isoya, A. Gali, M. Bockstedte, N. Morishita, T. Ohshima, and H. Itoh, Phys. Rev. Lett. **96**, 055501 (2006).

[24]P. G. Baranov, I. V. Ilyin, A. A. Soltamova, and E. N. Mokhov, Phys. Rev. B **77**, 085120 (2008).
[25]T. Umeda, J. Isoya, N. Morishita, T. Ohshima, E. Janzén, and A. Gali, Phys. Rev. B **79**, 115211 (2009).
[26]T. Umeda, J. Ishoya, T. Ohshima, N. Morishita, H. Itoh, and A. Gali, Phys. Rev. B **75**, 245202 (2007).
[27]T. Umeda, N. T. Son, J. Isoya, N. Morishita, T. Ohshima, H. Itoh, and E. Janzén, Mater. Sci. Forum **527-529**, 543 (2006).
[28]U. Gerstmann, A. P. Seitsonen, D. Ceresoli, F. Mauri, H. J. von Bardeleben, J. L. Cantin, and J. Garcia Lopez, Phys. Rev. B **81**, 195208 (2010).
[29]H. Itoh, M. Yoshikawa, I. Nishiyama, S. Misawa, H. Okumura, and S. Yoshida, IEEE Trans. Nucl. Sci. **37**, 1732 (1990).
[30]H. Itoh, M. Yoshikawa, I. Nashiyama, S. Misawa, H. Okumura, and S. Yoshida, J. Electron. Mater. **21-7**, 707 (1992).
[31]H. Itoh, A. Uedono, T. Ohshima, Y. Aoki, M. Yoshikawa, I. Nashiyama, S. Tanigawa, H. Okumura, and S. Yoshida, Appl. Phys. A Mat. Sci. Proc. **65**, 315 (1997).
[32]N. T. Son, E. Janzen, J. Isoya, N. Morishita, H. Hanaya, H. Takizawa, T. Ohshima, and A. Gali, Phys. Rev. B **80**, 125201 (2009).
[33]J. Lefèvre, J. M. Costantini, S. Esnouf, and G. Petite, J. Appl. Phys. **105**, 023520 (2009).
[34]R. Devanathan, and W. J. Weber, J. Nucl. Mater. **278**, 258 (2000).
[35]D. Lesueur, Philos. Mag. A **44**, 905 (1981).
[36]J. Baro, J. Sempau, J. M. Fernandez-Varea, and F. Salvat, Nucl. Instrum. Methods Phys. Res., Sect. B **100**, 31 (1995).
[37]Y. Goldberg, M. Levinshtein, and S. L. Rumyantsev, in *Properties of Advanced Semiconductor Materials GaN, AlN, SiC, BN, SiGe*, edited by M. E. Levinshtein, S. L. Rumyantsev, and M. S. Shur (Wiley, New York, 2001), p. 93.
[38]P. Edel, C. Hennies, Y. Merle d'Aubigné, R. Romestain, and Y. Twarowski, Phys. Rev. Lett. **28**, 1268 (1972).
[39]M. Bockstedte, M. Heid, and O. Pankratov, Phys. Rev. B **67**, 193102 (2003).
[40]P. Deak, J. Miro, A. Gali, L. Udvardi, and H. Overhof, Appl. Phys. Lett. **75**, 2103 (1999).
[41]M. Bockstedte, A. Mattausch, and O. Pankratov, Phys. Rev. B **68**, 205201 (2003).
[42]L. Wenchang, Z. Kaiming, and X. Xide, J. Phys. Condens. Matter **5**, 891 (1993).
[43]L. Torpo, S. Pöykkö, and R. M. Nieminen, Phys. Rev. B **57**, 6243 (1998).
[44]A. Zywietz, J. Furthmüller, and F. Bechstedt, Phys. Rev. B **59**, 15166 (1999).
[45]B. Aradi, A. Gali, P. Deak, J. E. Lowther, N. T. Son, E. Janzen, and W. J. Choyke, Phys. Rev. B **63**, 245202 (2001).
[46]A. Gali, P. Deak, P. Ordejon, N. T. Son, E. Janzen, and W. J. Choyke, Phys. Rev. B **68**, 125201 (2003).
[47]M. Bockstedte, A. Marini, A. Gali, O. Pankratov, and A. Rubio, Phys. Status Solidi B - Basic Solid State Phys. **245**, 1281 (2008).
[48]G. D. Watkins, in *Deep Centers in Semiconductors*, edited by S. T. Pantelides (Gordon and Breach, New York, 1986), p. 147.